# Polaron effect on the optical rectification in spherical quantum dots with electric field*

Zhen-Yu Feng(冯振宇)[1] and Zu-Wei Yan(闫祖威)[1,2,†]

[1] School of Physical Science and Technology, Inner Mongolia University, Hohhot 010021, China
[2] College of Science, Inner Mongolia Agricultural University, Hohhot 010018, China

(Received 27 February 2016; revised manuscript received 30 May 2016; published online 25 August 2016)

The polaron effect on the optical rectification in spherical quantum dots with a shallow hydrogenic impurity in the presence of electric field is theoretically investigated by taking into account the interactions of the electrons with both confined and surface optical phonons. Besides, the interaction between impurity and phonons is also considered. Numerical calculations are presented for typical $Zn_{1-x}Cd_xSe/ZnSe$ material. It is found that the polaronic effect or electric field leads to the redshifted resonant peaks of the optical rectification coefficients. It is also found that the peak values of the optical rectification coefficients with the polaronic effect are larger than without the polaronic effect, especially for smaller Cd concentrations or stronger electric field.

**Keywords:** polaron effect, optical rectification, spherical quantum dot

**PACS:** 78.67.Hc, 73.21.La, 71.38.–k **DOI:** 10.1088/1674-1056/25/10/107804

## 1. Introduction

Nonlinear optical properties in low-dimensional semiconductor nanostructures such as quantum wells, quantum wires, and quantum dots (QDs) have aroused much interest in the past few years.[1–16] In these systems, QDs can confine charge carriers in all spatial dimensions and their sizes, shapes, and other properties can be controlled experimentally. Furthermore, there exists a strong quantum confinement effect in QDs, which induces a dramatic enhancement in optical nonlinearities compared with bulk materials. This property leads to potential applications in electronic and optoelectronic devices.[17–19] Therefore, it is necessary to study the nonlinear optical properties of QDs due to their unique physical properties and their potential applications.

Because the electron–phonon interaction plays an important role in the nonlinear optical properties, the polaron effects on linear and nonlinear optical properties have been widely studied.[20–25] In nonlinear optical properties, nonlinear optical rectification (OR) in semiconductor heterostructure and nanostructure is a second-order nonlinear optical effect which is important for investigating their electronic structures. Due to the fact that the polaron effect can induce a very large enhancement effect, a lot of authors have devoted themselves to the issue about the polaron effect on the OR coefficient. For instance, Zhang and Guo[26] investigated the effect of the electron–phonon interaction on the OR in a semi-parabolic quantum well and found that the electron–phonon interaction increases the OR up to a factor of 6–13. Wu *et al.*[27] investigated the polaron effect on nonlinear OR in asymmetrical Gaussian potential quantum well, and revealed that the OR coefficients are strongly dependent on the confinement potential and the electric field, and greatly enhanced by considering the polaron effect. Xiao *et al.*[28] investigated the polaron effect on the OR in an asymmetrical semi-exponential quantum well, and they reported that when considering the electron-LO-phonon, the resonant peak of the OR is enhanced, and the blue shifts are also observed. Liu *et al.*[29,30] studied the polaron effect on the OR in cylindrical quantum dots in the presence of electric and magnetic fields and found that the OR coefficient is greatly enhanced, with the polaron effect taken into account. All relative research results reveal that electron–phonon interaction plays a very important role in nonlinear optical properties.

Due to the difference in the dielectric constant of the material between inside and outside the QDs, besides the confined optical (CO) phonons, there exist surface optical (SO) phonons in the structure, and it depends strongly on the QD shape and electric field.[31] In some investigations, the QD shapes were approximated as various forms: cylinders,[29,30] cones,[32] lens,[33,34] pyramids,[35] ellipses,[36,37] spheres,[38–40] and the polaronic effect has been studied in some works. Unfortunately, in most of the research mentioned above the impurity–phonon interaction is either ignored or not discussed. In fact, the contribution from impurity–phonon interaction is very important and generally larger than that from electron–phonon interaction.[41,42] To the best of our knowledge, there are fewer

*Project supported by the National Natural Science Foundation of China (Grant No. 11364028), the Major Projects of the Natural Science Foundation of Inner Mongolia Autonomous Region, China (Grant No. 2013ZD02), and the Project of "Prairie Excellent" Engineering in Inner Mongolia Autonomous Region, China.

†Corresponding author. E-mail: zwyan101@126.com

© 2016 Chinese Physical Society and IOP Publishing Ltd 

research studies related to the polaron effect on the OR in spherical quantum dots with taking into account both electron–phonon and impurity–phonon interaction. For these reasons, the polaron effect is important to the OR of QDs and should be considered in the relevant work.

In this paper, polaron effect on the OR in a spherical quantum dot in the presence of the electric field is theoretically investigated by using a variational approach, with the electron–phonon and impurity–phonon interactions taken into account, including CO and SO phonon modes. To make it closer to the real situation, the electronic confinement is modeled by a finite potential well. The rest of this paper is organized as follows. In Section 2, the electron–phonon interaction and the nonlinear OR coefficients are described. In Section 3, the numerical results and discussions are performed. Finally, some conclusions are briefly drawn from the present study in Section 4.

## 2. Model and calculation

We consider the electron interacting with the optical phonons in a spherical quantum dot comprised of $Zn_{1-x}Cd_xSe/ZnSe$ with radius $R$. When the electron is inside ($r < R$) the QD, it will interact with the internal LO phonons, we call it CO phonons. When the electron is close to the QD boundary ($r \approx R$), it will interact with the SO phonons. Within the framework of effective mass approximation, the Hamiltonian of the system in the presence of an applied electric field along the $z$ direction is given by

$$H = H_0 + H_{\rm ph}^{\rm CO} + H_{\rm ph}^{\rm SO} + H_{\rm ep}^{\rm CO} + H_{\rm ep}^{\rm SO}. \tag{1}$$

Here, $H_0$ is the Hamiltonian of the electron, which can be written as

$$H_0 = \frac{p^2}{2m} - \frac{e_{\rm s}^2}{\varepsilon r} + U(\boldsymbol{r}) + |e|Fr\cos\theta, \tag{2}$$

with

$$U(\boldsymbol{r}) = \begin{cases} 0, & \text{for } r \le R, \\ U_0, & \text{for } r > R, \end{cases}$$

$$m = \begin{cases} m_1, & \text{for } r < R, \\ m_2, & \text{for } r > R, \end{cases}$$

$$\varepsilon = \begin{cases} \varepsilon_{1\infty}, & \text{for } r < R, \\ (\varepsilon_{1\infty} + \varepsilon_{2\infty})/2, & \text{for } r > R, \end{cases} \tag{3}$$

where $m_1$ ($m_2$) and $\varepsilon_{1\infty}$ ($\varepsilon_{2\infty}$) are the effective mass and high-frequency dielectric constant in dot (barrier) material respectively, $F$ is the strength of the electric field along the $z$ direction, $U(\boldsymbol{r})$ is the confinement potential of the spherical QD, $e_{\rm s} = e/(4\pi\varepsilon_0)^{-1/2}$, and $e$ is absolute value of the electron charge, and $\varepsilon_0$ is the vacuum permittivity, $\theta$ is the angle between the electronic position vector $\boldsymbol{r}$ and the electric field direction. The second and third term in Eq. (1) representing the classical Hamilton functions of CO and SO phonons can be written respectively as follows:

$$H_{\rm ph}^{\rm CO} = \sum_{lmn} \hbar\omega_{\rm CO}\left(a_{lmn}^{\dagger}a_{lmn} + \frac{1}{2}\right), \tag{4}$$

$$H_{\rm ph}^{\rm SO} = \sum_{lm} \hbar\omega_{{\rm SO},l}\left(a_{lm}^{\dagger}a_{lm} + \frac{1}{2}\right), \tag{5}$$

where $\omega_{\rm CO}$ and $\omega_{{\rm SO},l}$ are the eigenfrequencies of CO and SO phonons respectively. $H_{\rm ep}^{\rm CO}$ and $H_{\rm ep}^{\rm SO}$ in Eq. (1) are the Hamiltonian of both electron and impurity interaction with CO and SO phonons, which can be expressed as[43,44]

$$H_{\rm ep}^{\rm CO} = -\sum_{lmn} \beta_{lmn}^{\rm CO}\left\{\left[V_{lmn}^{\rm CO}(r) - V_{lmn}^{\rm CO}(r_0)\right]a_{lmn} + {\rm H.c.}\right\}, \tag{6}$$

$$H_{\rm ep}^{\rm SO} = \begin{cases} -\sum\limits_{lm} \beta_{lm}^{\rm SO}\left\{\left[V_{lm}^{\rm SO}(r) - V_{lm}^{\rm SO}(r_0)\right]a_{lm} + {\rm H.c.}\right\}, & r < R, \\ -\sum\limits_{lm} \beta_{lm}^{\rm SO}\left[V_{lm}^{\rm SO}(r)a_{lm} + {\rm H.c.}\right], & r > R, \end{cases} \tag{7}$$

where

$$\beta_{lmn}^{\rm CO} = \left\{\frac{4\pi e_{\rm s}^2}{R}\frac{\hbar\omega_{\rm CO}}{\mu_{ln}^2 {\rm j}_{l+1}^2(\mu_{ln})}\left(\frac{1}{\varepsilon_{1\infty}} - \frac{1}{\varepsilon_{10}}\right)\right\}^{1/2}, \tag{8}$$

with

$$V_{lmn}^{\rm CO}(r) = {\rm j}_l(k_{ln}r){\rm Y}_{lm}(\theta,\varphi), \tag{9}$$

and

$$\beta_{lm}^{\rm SO} = \frac{\varepsilon_{1\infty}\sqrt{l}}{l\varepsilon_{1\infty} + (l+1)\varepsilon_d}\omega_{\rm CO}\sqrt{\frac{2\pi e_{\rm s}^2\hbar}{\omega_{{\rm SO},l}R}\left(\frac{1}{\varepsilon_{1\infty}} - \frac{1}{\varepsilon_{10}}\right)}, \tag{10}$$

with

$$\omega_{{\rm SO},l}^2 = \frac{[\varepsilon_d + (\varepsilon_d + \varepsilon_{10})l]\varepsilon_{1\infty}}{[\varepsilon_d + (\varepsilon_d + \varepsilon_{1\infty})l]\varepsilon_{10}}\omega_{\rm CO}^2, \tag{11}$$

$$V_{lm}^{\rm SO}(r) = \begin{cases} (r/R)^l {\rm Y}_{lm}(\theta,\varphi), & r < R, \\ (R/r)^{l+1}{\rm Y}_{lm}(\theta,\varphi), & r > R, \end{cases} \tag{12}$$

where ${\rm Y}_{l,m}$ is the spherical harmonic, ${\rm j}_l$ and ${\rm n}_l$ are the $l$-th order spherical Bessel and Neumann functions respectively, $k_{ln} = \mu_{ln}/R$, $\mu_{ln}$ is the $n$-th root of ${\rm j}_l$, $\varepsilon_{1\infty}$ ($\varepsilon_{2\infty}$) and $\varepsilon_{10}$ ($\varepsilon_{20}$) are the high-frequency and static dielectric constants in dot (barrier) material respectively. The index $n = 1,2,\ldots$; $l = 0,1,2,\ldots$; $m = 0,\pm1,\pm2,\ldots,\pm l$ for the CO phonons, and $l = 1,2,\ldots$; $m = 0,\pm1,\pm2,\ldots,\pm l$ for the SO phonons. In Eqs. (6) and (7), $r$ and $r_0$ are the positions of electron and impurity respectively. In this paper, we assume that the impurity is in the center (the center of the sphere is taken as the origin), i.e., $r_0 = 0$.

Firstly, it is necessary to eliminate the contribution of the impurity–phonon interactions to the total electron energy. It can be obtained by using a first unitary transformation to displace the equilibrium position of the ions as follows:

$$U = \exp\left\{\sum_{j={\rm CO,SO}}\sum_{\rm s}\left[\frac{\beta_{\rm s}^j V_{\rm s}^j(r_0)a_{js}^{\dagger} + {\rm H.c.}}{\hbar\omega_j}\right]\right\}. \tag{13}$$

Here CO and SO represent the CO and SO phonons respectively. The index $s$ is given by $n = 1,2,\ldots$; $l = 0,1,2,\ldots$; $m = 0,\pm1,\pm2,\ldots,\pm l$ for the CO phonons, and $l = 1,2,\ldots$; $m = 0,\pm1,\pm2,\ldots,\pm l$ for the SO phonons.

Subsequently, the Hamiltonian can be transformed into the following form:

$$H^* = U^{-1}HU = H_0 + H_{\rm ph}^{\rm CO} + H_{\rm ph}^{\rm SO} + H'_{\rm ep,CO} + H'_{\rm ep,SO} + H_x, \quad (14)$$

where

$$H'_{\rm ep,CO} = -\sum_{lmn} \beta_{lmn}^{\rm CO} \left[ V_{lmn}^{\rm CO}(r) a_{lmn} + {\rm H.c.} \right], \quad (15)$$

and

$$H'_{\rm ep,SO} = -\sum_{lm} \beta_{lm}^{\rm SO} \left[ V_{lm}^{\rm SO}(r) a_{lm} + {\rm H.c.} \right]. \quad (16)$$

The nonphysical divergent term arising from the use of the point-charge model has been dropped for convenience, the effect of the above displacement on the lattice polarization leads to the following electron-impurity "exchange" interaction:

$$H_x = \sum_{j={\rm CO,SO}} \sum_{\rm s} \frac{|\beta_{\rm s}^j|^2 V_{\rm s}^j(r_0) V_{\rm s}^j(r) + {\rm H.c.}}{\hbar\omega_j}. \quad (17)$$

The effect of the electron–phonon interaction is to displace further the equilibrium positions of the ions within the adiabatic approximation. This can be obtained by the following unitary transformation:

$$U' = \exp\left\{ \sum_{j={\rm CO,SO}} \sum_{\rm s} \left[ f_{js} a_{js}^\dagger + {\rm H.c.} \right] \right\}. \quad (18)$$

The parameters $f_{js}$ are variational functions, which will be determined by minimizing the expectation value of the bound polaron energy. The total wave function of the system can be achieved by the product of the electronic part $|\varphi(\boldsymbol{r})\rangle$ and the phonon part $U'|0\rangle$[45]

$$|\psi\rangle = |\varphi(\boldsymbol{r})\rangle U'|0\rangle, \quad (19)$$

$$\varphi(r) = \begin{cases} N \dfrac{\sin k_{10} r}{r} f(r) & r \le R, \\ N \dfrac{\sin k_{10} R}{r} {\rm e}^{\chi_{10}(R-r)} f(r), & r \ge R, \end{cases} \quad (20)$$

$$f(r) = \begin{cases} {\rm e}^{-\lambda_1 r} {\rm e}^{-\eta_1 r\cos\alpha} & \text{for the ground state,} \\ r\cos\theta\, {\rm e}^{-\lambda_2 r} {\rm e}^{-\eta_2 r\cos\alpha} & \text{for the first excited state,} \end{cases} \quad (21)$$

with

$$k_{10} = \left( \frac{2m_1 E_{10}}{\hbar^2} \right)^{1/2}, \quad (22)$$

$$\chi_{10} = \left( \frac{2m_2 (U_0 - E_{10})}{\hbar^2} \right)^{1/2}, \quad (23)$$

where $N$ is the normalization constant; $\lambda_1$ ($\lambda_2$) and $\eta_1$ ($\eta_2$) are the variational parameters for the ground (excited) state, and indicate the degree of spatial correlation between the electron and impurity and the influence of the electric field, respectively; $E_{10}$ is the energy of the ground state achieved by the transcendental equation:

$$\frac{1}{m_1}\left( \frac{k_{10}}{\tan(k_{10}R)} - \frac{1}{R} \right) = \frac{1}{m_2}\left( -\frac{1}{R} - \chi_{10} \right). \quad (24)$$

After some calculations, the expectation value of the system Hamiltonian in the phonon–vacuum state is given by

$$\begin{aligned} H_{\rm eff} &= \langle 0| U'^{-1} H^* U' |0\rangle \\ &= H_0 + H_x + \sum_{j={\rm CO,SO}} \sum_{\rm s} \hbar\omega_j \left| f_{js} \right|^2 \\ &\quad + \sum_{j={\rm CO,SO}} \sum_{\rm s} \left[ \beta_{\rm s}^j V_{\rm s}^j(r) f_{js} + {\rm H.c.} \right]. \end{aligned} \quad (25)$$

Then, the minimization of the expectation energy value can be written as

$$E = \langle \varphi(\boldsymbol{r}) | H_{\rm eff} | \varphi(\boldsymbol{r}) \rangle, \quad (26)$$

with respect to the variational parameters $f_{js}$, which is given by the following expressions:

$$f_{js} = \begin{cases} -\dfrac{\langle \varphi(\boldsymbol{r}) | V_{lmn}^{\rm CO} | \varphi(\boldsymbol{r}) \rangle}{\hbar\omega_{\rm CO}} & \text{for CO phonon,} \\ -\dfrac{\langle \varphi(\boldsymbol{r}) | V_{lm}^{\rm SO} | \varphi(\boldsymbol{r}) \rangle}{\hbar\omega_{\rm SO}} & \text{for SO phonon.} \end{cases} \quad (27)$$

Finally, inserting Eqs. (25) and (27) into Eq. (26), and the expectation energy $E$ dependent on the variational parameters can be obtained in the form of

$$\begin{aligned} &E(\lambda,\eta) \\ &= \langle \varphi(\boldsymbol{r}) | H_0 | \varphi(\boldsymbol{r}) \rangle - \sum_{j={\rm CO,SO}} \sum_{\rm s} \left| \beta_{\rm s}^j \right|^2 \frac{|\langle \varphi(\boldsymbol{r}) | V_{\rm s}^j(r) | \varphi(\boldsymbol{r}) \rangle|^2}{\hbar\omega_j} \\ &\quad + \sum_{j={\rm CO,SO}} \sum_{\rm s} 2 \left| \beta_{\rm s}^j \right|^2 \frac{|\langle \varphi(\boldsymbol{r}) | V_{\rm s}^j(r) V_{\rm s}^j(r_0) | \varphi(\boldsymbol{r}) \rangle|}{\hbar\omega_j}. \end{aligned} \quad (28)$$

In this expression, the first term on the right-hand side indicates the energy of the impurity state, the second term describes the interactions of the electron with both CO and SO phonons, and the last term describes the electron–impurity "exchange" interaction caused by the impurity–phonon interaction.

The analytical expression for the nonlinear optical rectification coefficient can be obtained by a density matrix approach and an iterative procedure[46,47]

$$\begin{aligned} \chi_0^{(2)} &= \frac{4q^3\sigma}{\varepsilon_0\hbar^2} M_{12}^2 \delta_{12} \\ &\quad \times \frac{\omega_{12}^2(1+\Gamma_2/\Gamma_1) + (\omega^2+\Gamma_2^2)(\Gamma_2/\Gamma_1 - 1)}{[(\omega_{12}-\omega)^2+\Gamma_2^2][(\omega_{12}+\omega)^2+\Gamma_2^2]}, \end{aligned} \quad (29)$$

where $q$ is the absolute value of the electron charge, $\sigma$ denotes the electron density in the system, $\Gamma_i$ ($i = 1,2$) is the phenomenological relaxation rate, $\Gamma_1 = 1/T_1$, and $\Gamma_2 = 1/T_2$, with

$T_1$ and $T_2$ being the longitudinal and the transverse relaxation times, respectively, $M_{12} = \langle \varphi_1 | z | \varphi_2 \rangle$ is the dipole matrix element, $\delta_{12} = |\langle \varphi_2 | z | \varphi_2 \rangle - \langle \varphi_1 | z | \varphi_1 \rangle|$, $\hbar\omega_{12} = E_2 - E_1$ is the energy difference between two different electronic states, and $\omega$ is the incident photon frequency.

The maximum value of $\chi_0^{(2)}$ for $\omega_{12} = \omega$ is given by

$$\chi_{0,\max}^{(2)} = \frac{2q^3 T_1 T_2 \sigma}{\varepsilon_0 \hbar^2} M_{12}^2 \delta_{12}. \tag{30}$$

## 3. Results and discussion

In this section, we will discuss the OR coefficients in a spherical quantum dot with the electric field in the presence of the electron–phonon and impurity–phonon interactions. The parameters used in our calculations are as follows:[48–50] $\sigma = 5.0 \times 10^{24}$ m$^{-3}$, $n_r = 2.4$, $T_1 = 1$ ps, $T_2 = 0.1$ ps; $m_1 = 0.13m_0$, $\varepsilon_{10} = 9.3$, $\varepsilon_{1\infty} = 6.1$ for CdSe; $m_1 = 0.171m_0$, $\varepsilon_{10} = 8.33$, $\varepsilon_{1\infty} = 5.9$, $\varepsilon_d = 2.25$ for ZnSe, where $m_0$ is the bare electron mass. The parameters for $Zn_{1-x}Cd_xSe$ are obtained by linear interpolation from the corresponding values for ZnSe and CdSe. The value of the conduction band offset $U_0$ is assumed to be 80% of bandgap mismatch.[43]

In Fig. 1, we demonstrate the behaviors of OR coefficient $\chi_0^{(2)}$ in the cases with and without phonon, each as a function of photon energy $\hbar\omega$ for different QD radii with $F = 5.0$ MV/m and $x = 0.3$. From the figure, it can be clearly seen that the polaronic effect gives rise to the redshifts of the positions of the resonant peaks of the OR coefficients, especially for the smaller QD radius. We find that the redshifts for the OR coefficient are 6.5 meV, 3.5 meV, 2.5 meV for $R = 4$ nm, 6 nm, and 8 nm, respectively. Besides, a very notable feature of this figure is that when we take into account the polaronic effect, the peak values of the OR coefficient $\chi_0^{(2)}$ are enhanced. The reason for this feature is that the polaronic effect makes the wave function of an electron spread to wider space, which leads to the fact that the overlap of the wave functions is enhanced.

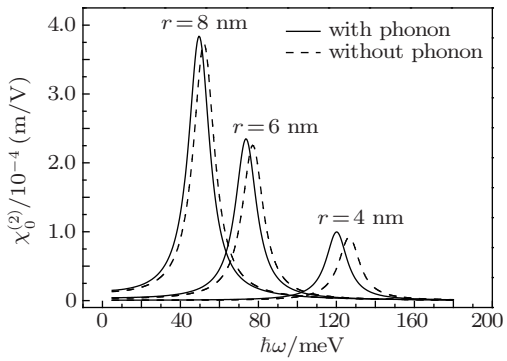



**Fig. 1.** Variations of OR coefficient $\chi_0^{(2)}$ with photon energy $\hbar\omega$ with and without phonon for different QD radii with $F = 5.0$ MV/m and $x = 0.3$.

Figure 2 shows the OR coefficients $\chi_0^{(2)}$ with and without phonon each as a function of photon energy $\hbar\omega$ for different Cd concentrations with $F = 2.0$ MV/m, and $R = 5$ nm. It can also be seen that the polaronic effect leads to the redshifted resonant peaks of the OR coefficients. We find that the redshifts for the OR coefficient are 7.0 meV, 5.5 meV, and 3.5 meV for $x = 0.1$, 0.2, and 0.5, respectively. Moreover, from the figure, we can obviously observe that the peak values of $\chi_0^{(2)}$ with the polaronic effect are larger than without the polaronic effect, especially for the smaller Cd concentrations. Furthermore, it is found that the peak values of $\chi_0^{(2)}$ decrease with increasing Cd concentration. In order to explain the feature, we show the relationship between the geometrical factor $M_{12}^2\delta_{12}$ and the Cd concentration $x$ with $F = 2.0$ MV/m and $R = 5$ nm in Fig. 3. We know that the resonant peak of $\chi_0^{(2)}$ is determined by the geometrical factor $M_{12}^2\delta_{12}$. From the figure, it is obviously seen that the geometrical factor $M_{12}^2\delta_{12}$ decreases with $x$ increasing. In addition, the geometrical factor difference between the two cases gradually becomes small with increasing Cd concentration. These results are useful for understanding the results in Fig. 2. Finally, it should be pointed out that from Fig. 2, whether the polaronic effect is considered or not, the peak value of $\chi_0^{(2)}$ suffers a blue-shift with increasing Cd concentration. The reason for the feature is that with increasing Cd concentration, the confinement potential strengthens, and as a result, the quantum-confinement of the electron is enhanced. Therefore, the energy intervals are much wider, which leads to the fact that the positions of $\chi_0^{(2)}$ peaks appear on the higher-energy side.

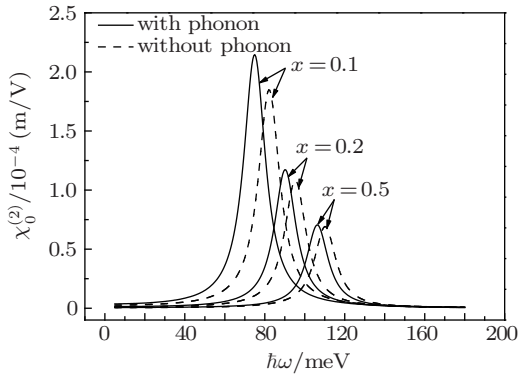



**Fig. 2.** Plots of OR coefficients $\chi_0^{(2)}$ versus photon energy $\hbar\omega$ with and without phonon for different Cd concentrations with $F = 2.0$ MV/m and $R = 5$ nm.

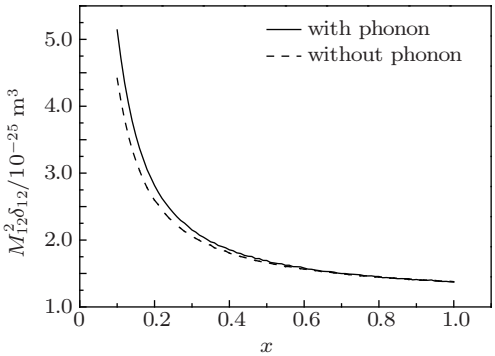



**Fig. 3.** Variations of geometrical factor $M_{12}^2\delta_{12}$ with Cd concentration $x$ with and without phonon for $F = 2.0$ MV/m and $R = 5$ nm.

Figure 4 shows variations of the OR coefficient $\chi_0^{(2)}$ with photon energy $\hbar\omega$ with and without phonon for different electric fields with $R = 5$ nm, and $x = 0.3$. From the figure, it is clearly observed that the electric field $F$ also leads to the redshifted resonant peaks of the OR coefficients and enhances its peak values. The enhancement of the $\chi_0^{(2)}$ peak can be attributed to the increase of the asymmetry of the system and the enhancement of the geometrical factor $M_{12}^2\delta_{12}$. The redshift of the $\chi_0^{(2)}$ peak is attributed to the decrease of energy difference between the ground and excited states with increasing electric field $F$. In addition, from the figure, we also observe that the peak values of $\chi_0^{(2)}$ with the polaronic effect are larger than without the polaronic effect, which is more obvious with increasing $F$. In order to show the relationship between the peak value of $\chi_0^{(2)}$ and the electric field $F$, the geometrical factor $M_{12}^2\delta_{12}$ versus electric field is plotted in Fig. 5. From the figure, it is clearly seen that the geometrical factor $M_{12}^2\delta_{12}$ increases with electric field $F$ increasing. This is due to the fact that the increase of $F$ weakens the spatial separation of particles and causes an enhancement of the overlap between their associated wave functions. Furthermore, the geometrical factor difference between the two cases is enhanced with increasing $F$. This feature has good consistency with the results in Fig. 4.

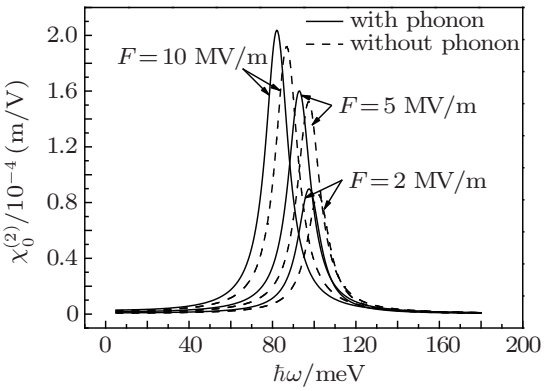



**Fig. 4.** Variations of OR coefficient $\chi_0^{(2)}$ with photon energy $\hbar\omega$ with and without phonon for different electric fields with $R = 5$ nm and $x = 0.3$.

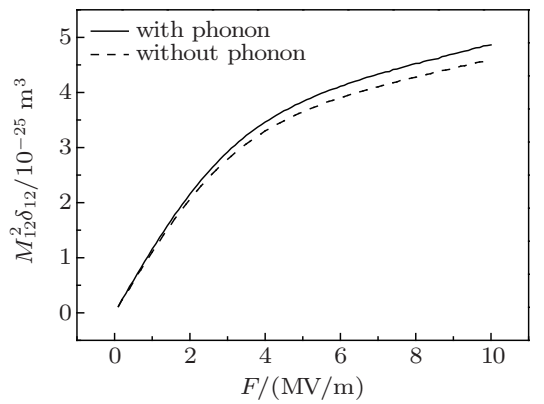



**Fig. 5.** Plots of geometrical factor $M_{12}^2\delta_{12}$ versus electric field $F$ with and without phonon for $x = 0.3$ and $R = 5$ nm.

## 4. Conclusions

In this paper, we study theoretically the polaron effect on the OR in a $Zn_{1-x}Cd_xSe/ZnSe$ spherical quantum dot with electric field in detail, with the electron–phonon and impurity–phonon interactions taken into account. Our calculations mainly focus on the dependences of the OR on external electric field $F$, Cd concentration $x$, and QD radius $R$. The calculated results show that the polaronic effect or electric field leads to the redshifted resonant peaks of the OR coefficients. Our result also reveals that the peak values of $\chi_0^{(2)}$ with the polaronic effect are larger than without the polaronic effect, especially for smaller Cd concentrations or stronger electric field. In addition, whether the polaronic effect is considered or not, the peak value of $\chi_0^{(2)}$ decreases and suffers a blueshift with increasing Cd concentration. It should be pointed out that the external LO phonon is ignored in this work since its influence is very small and only effective for the very small dot size.[31,43] Finally, we hope that this theoretical study can make a significant contribution to experimental studies and practical applications.

## References


[1] Hai G Q, Peeters F M and Devreese J T 1993 *Phys. Rev. B* **47** 10358
[2] Kasapoglu E and Sari H 2001 *Superlatt. Microstruct.* **29** 25
[3] Li B, Guo K X, Zhang C J and Zheng Y B 2007 *Phys. Lett. A* **367** 493
[4] Atanasov R, Bassani F and Agranovich V M 1994 *Phys. Rev. B* **50** 7809
[5] Ozturk E and Sökmen I 2004 *Eur. Phys. J. Appl. Phys.* **25** 3
[6] Karabulut I and Baskoutas S 2008 *J. Appl. Phys.* **103** 073512
[7] Liu G, Guo K and Wang C 2012 *Physica B* **407** 2334
[8] Prasad V and Silotia P 2011 *Phys. Lett. A* **375** 3910
[9] Wang G H 2005 *Phys. Rev. B* **72** 155329
[10] Yesilgul U 2012 *J. Lumin.* **132** 765
[11] Ungan F, Martínez-Orozco J C, Restrepo R L, Mora-Ramos M E, Kasapoglu E and Duque C A 2015 *Superlatt. Microstruct.* **81** 26
[12] Kasapoglu E, Duque C A, Mora-Ramos M E and Sökmen I 2015 *Physica B* **474** 15
[13] Jbara A S, Othaman Z and Saeed M A 2016 *Chin. Phys. B* **25** 057801
[14] Karabulut I and Paspalakis E 2016 *Physica E* **81** 294
[15] She Y C, Luo T T, Zhang W X, Ran M W and Wang D L 2016 *Chin. Phys. B* **25** 014202
[16] Ghosh A P, Mandal A, Sarkar S and Ghosh M 2016 *Opt. Commun.* **367** 325
[17] Troccoli M, Belyamin A, Capasso F, Cubukcu E, Sivco D L and Cho A Y 2005 *Nature* **433** 845
[18] Leobandung E, Guo L, Wang Y and Chou S Y 1995 *Appl. Phys. Lett.* **67** 938
[19] Phillips J 2002 *J. Appl. Phys.* **91** 4590
[20] Yu Y B, Zhu S N and Guo K X 2006 *Solid State Commun.* **139** 76
[21] Xie W F 2011 *Physica B* **406** 2858
[22] Li N, Guo K X and Shao S 2011 *Superlatt. Microstruct.* **49** 468
[23] Shi L and Yan Z W 2015 *Solid State Commun.* **209** 27
[24] Senthil Kumar N R, John Peter A and Lee Chang Woo 2015 *J. Comput. Theor. Nanosci.* **12** 916
[25] Khordad R and Bahramiyan H 2015 *Opt. Quantum Electron.* **47** 2727
[26] Zhang C J and Guo K X 2007 *Physica B* **387** 276
[27] Wu J H, Guo K X and Liu G H 2014 *Physica B* **446** 59
[28] Xiao B, Guo K X and Zhang Z M 2014 *Superlatt. Microstruct.* **69** 122
[29] Liu G H, Guo K X, Wu Q J and Wu J H 2013 *Superlatt. Microstruct.* **53** 173
[30] Liu G H, Guo K X and Wu J H 2013 *Superlatt. Microstruct.* **57** 102
[31] Shi L and Yan Z W 2013 *Eur. Phys. J. B* **86** 244

[32] Margin J Y and Bastard G 1994 *Solid State Commun.* **92** 437
[33] Bouzaïene L, Ben Mahrsia R, Baira M, Sfaxi L and Maaref H 2013 *J. Lumin.* **135** 271
[34] Ben Mahrsia R, Choubani M, Bouzaiene L and Maaref H 2016 *J. Alloys Compd.* **671** 200.
[35] Roy M and Masym P A 2003 *Phys. Rev. B* **68** 235308
[36] Chen T R, Xie W F and Liang S J 2012 *Physica E* **44** 786
[37] Giraldo-Tobón E, Ospina W, Miranda-Pedraza G L and Mora-Ramos M E 2015 *Superlatt. Microstruct.* **83** 157
[38] Xie H J and Chen C Y 1998 *Eur. Phys. J. B* **5** 215
[39] Oshiro K, Akai K and Matsuura M 2002 *Phys. Rev. B* **66** 153308
[40] Vaseghi B, Sadri M, Rezaei G and Gharaati A 2015 *Physica B* **457** 212
[41] Shi L and Yan Z W 2011 *J. Appl. Phys.* **110** 024306
[42] Huang Fu Y F and Yan Z W 2008 *Physica E* **40** 2982
[43] Melnikov D V and Fowler W B 2001 *Phys. Rev. B* **64** 245320
[44] Klein M C, Hache F, Ricard D and Flytzanis C 1990 *Phys. Rev. B* **42** 11123
[45] Daries Bella R S and Navaneethakrishnan K 2004 *Solid State Commun.* **130** 773
[46] Guo K X and Gu S W 1993 *Phys. Rev. B* **47** 16322
[47] Wang R Z, Guo K X, Liu Z L, Chen B and Zheng Y B 2009 *Phys. Lett. A* **373** 795
[48] Christina P, Jasmine Lily, John Peter A and Lee Chang Woo 2014 *Phys. Scr.* **89** 085805
[49] Wang S Y, Kawakami Y, Simpson J, Stewart H, Prior K A and Cavenett B C 1993 *Appl. Phys. Lett.* **62** 1715
[50] Melnikov D V and Fowler W B 2001 *Phys. Rev. B* **64** 195335